



**Adhesion of Lactoferrin and Bone Morphogenetic Protein-2  
to a Rutile Surface: Dependence on the Surface  
Hydrophobicity.**

Journal:	<i>Biomaterials Science</i>
Manuscript ID:	BM-ART-01-2014-000021.R2
Article Type:	Paper
Date Submitted by the Author:	01-Apr-2014
Complete List of Authors:	Sun, Tianyang; chemsity, chemistry Han, Guang; Stockholm University, Materials and Environmental Chemistry Lindgren, Matteus; Boliden, Boliden Odda AS Shen, Zhijian; Stockholm University, Materials and Environmental Chemistry Laaksonen, Aatto; Stockholm University, Materials and Environmental Chemistry

**Adhesion of Lactoferrin and Bone Morphogenetic Protein-2 to a  
Rutile Surface:  
Dependence on the Surface Hydrophobicity.**

**Tianyang Sun**

Soft Matter Research Center and Department of Chemistry, Zhejiang University,  
310027 Hangzhou,  
P. R. China

Department of Materials and Environmental Chemistry, Arrhenius Laboratory,  
Stockholm University, S-106 91 Stockholm, Sweden

**Guang Han**

Department of Materials and Environmental Chemistry, Arrhenius Laboratory,  
Stockholm University, S-106 91 Stockholm, Sweden

**Matteus Lindgren**

Boliden Odda AS, NO-5750 Odda, Norway

**Zhijian Shen**, Department of Materials and Environmental Chemistry, Arrhenius  
Laboratory, Stockholm University, S-106 91 Stockholm, Sweden

**Aatto Laaksonen**

Department of Materials and Environmental Chemistry, Arrhenius Laboratory,  
Stockholm University, S-106 91 Stockholm, Sweden

**Abstract**

Binding of the proteins human LactoFerrin (LF) and human Bone Morphogenetic Protein-2 (BMP2) to hydroxylated TiO<sub>2</sub> rutile (110) surface has been modeled using Molecular Dynamics (MD) simulations. In order to study the effect of the hydrophobicity of the rutile surface on the protein binding process, the rutile surface was made more hydrophilic or more hydrophobic by adjusting the rutile atomic charges. The binding of LF and BMP2 to the hydrophobic rutile surface occurred through direct contact between the protein and rutile via both hydrophobic and hydrophilic amino acids. This forced the proteins to undergo structural rearrangements, observed primarily in BMP2. Binding to the hydrophilic rutile surface was largely indirect via the hydration layer of water on the surface of rutile. Both LF and BMP2 had a higher binding strength to the hydrophobic rutile surfaces than to the hydrophilic surfaces, as seen in the larger amplitude of the binding energies.

**Keywords:** Adhesion mechanism; BMP (bone morphogenetic protein); Molecular modelling; Titanium dioxide

## Introduction

Titanium materials are among the most commonly used biomaterials because of their good biocompatibility, machinability, corrosion resistance and Osseo integration and used in applications such as biomedical implants and biosensors. Titanium dioxide has been widely studied and used as a coating material, capable to protect the metal from further oxidation or induced apatite layer formation and to improve the capability of tissue binding with Ti and thereby better meet the clinical requirements. Direct contacts between  $\text{TiO}_2$  and proteins and cells from body fluids have an important effect on the biological response and biocompatibility for implants. Both experimental and computational studies in the past have improved the understanding of protein adsorption mechanism.[1] These have been helpful in the development of new materials for applications, such as biocompatible materials for biomedical devices inserted in living bodies, biosensors that can detect the presence of target proteins and purifiers that can absorb unwanted biological materials from a solution.

Computer simulations such as molecular dynamics (MD) have been used to study the protein adsorption on various biocompatible materials. MD is a powerful technique to elucidate the mechanisms behind protein-material interaction at atomic level giving information about specific structural dynamics. Many studies about the interaction of biomolecules and titanium dioxide have focused on perfectly smooth titanium surface. In these studies, protein/peptide conformational changes, specific binding sites, as well as contribution of water molecules in the binding to interface have been investigated and compared with other surfaces such as graphite or hydroxylapatite.[2-6] Previous studies established that protein-material interactions not only depend on the protein characteristics, such as size, charge, hydrophobicity, conformation, and stability, but also the surface characteristics of the materials (surface chemistry and topography), which is currently of great interest.[7, 8] Surface modifications by generating micro- or nano-porous structure and attaching functional groups or peptides [9-12] have been used to design suitable surfaces. Thus, more work needs to be devoted to studies how the different physicochemical nature of the surface modification affects the protein adsorption. Roach et al. [13] have compared protein adsorption onto model hydrophobic ( $\text{CH}_3$ ) and hydrophilic ( $\text{OH}$ ) gold-coated surfaces using quartz crystal microbalance and grazing angle infrared spectroscopy. The

binding rates, strength and protein bound conformation are influenced by different hydrophobicity. Molecular simulation studies on hydroxylated titanium dioxide surface suggested that the hydroxylated surface have a closer and stronger interaction with protein.[14] For the negatively charged rutile surface, it is indicated that the surface hydroxylation, mediated by water and cations, determined RGD peptide (Arg-Gly-Asp) adsorption where the ions in a micro-environment are also very important in protein-surface interactions.[15] These investigations are useful to alter protein/cell adhesion for the design of implants and for wound care products, but much more understanding is required in order to design biomaterials to meet the needs of different applications.

In this work, we have explored the effect of surface hydrophobicity of hydroxylated rutile (110) surface on the protein adsorption by MD simulations. Many proteins have been found to be able to interact with  $\text{TiO}_2$ , which is of great importance in the biological applications of this material. Herein, human LactoFerrin (LF) and human Bone Morphogenetic Protein-2 (BMP2) were chosen to describe the adsorption characteristics. LF is an iron-binding protein with 691 residues. It shows antibacterial activity in clinical studies.[16] BMP-2 is a disulfide-connected dimer in bioactive form, including 114 residues in each monomer. It has been proven to induce differentiation and proliferation of osteoblasts, which makes it indispensable for bone formation and regeneration. BMP-2, receiving approval of the US Food and Drug Administration (FDA) and the European Medicines Agency (EMA) for clinical use, is of great interests to improve its applications by understanding the mechanism of BMP-2-surface interaction. We have compared the adsorption patterns of these two model proteins with significantly different sizes and structures on surfaces with different hydrophobicity.

## **Methodology**

### **The Rutile surface**

A planar surface consisting of 5 layers of (110) rutile was built. This surface originates from dissociative adsorption of water onto the rutile structure, resulting in a complete coverage of the surface with hydroxyl groups. The hydroxyl group (Oth-Hth) of a water molecule binds to a surface Ti atom and the other hydrogen in water

(Hbp) binds to a bridging oxygen atom (Obp) of the rutile surface (see Figure.1). The Bandura and Kubicki potential [17] was used to describe the interactions for both molecular and dissociated water to surfaces of TiO<sub>2</sub>. The atomic charges and force field parameters were taken from the refinement work by Predota et al.[18] The neutral hydroxylated rutile (110) surface was built as described in ref.[18]. This rutile surface is denoted hereafter as “*original*” and the atomic charges are shown in Table 1. To study how the rutile surface hydrophobicity affects the binding of protein, two modified versions of the rutile surface were generated in addition to the *original* surface. The charges of all atoms of rutile, including the hydroxyl groups, were homogeneously scaled by a factor of 0.5 or 1.4 in order to produce one surface that was more hydrophobic and another surface that was more hydrophilic than the *original* surface, respectively. The surface was charge-neutral as a whole in all simulations. We denote these in this way modified rutile surfaces as “*low*” and “*high*”, respectively, where *low* is the most hydrophobic surface and *high* is the most hydrophilic surface.

### **Protein Structures**

The protein structure of lactoferrin (LF) was obtained from Protein Data Bank (ID: 1CB6). LF is an iron transfer protein consisting of two homologous globular domains named N-and C-lobes. Each lobe contains one iron binding site and one glycosylation site that are located on the opposite ends of the protein. Apo-LF without bound ions was simulated in this work with an opened N-lobe and a closed C-lobe.

The initial coordinates of BMP2, taken from Protein Data Bank (ID: 3BMP), were used to derive a homo-dimer with a covalent bond between the Cys78 residues of each monomer at <http://pqs.ebi.ac.uk>. However, residues 1 to 8 in the monomer are missing. They were therefore added as a linear structure to the protein where after that part of the protein was extensively equilibrated first in vacuum and thereafter in water. The equilibration resulted in folding of residues 1 to 8 of both monomers closer to the main part of the protein but they still lack direct contact.

### **Computational details**

All simulations were performed with the Gromacs 4.0.5 and Amber 03 all-atom force field supplemented by TiO<sub>2</sub> parameters.[18, 19] The proteins were solvated in TIP3P

water [20] in periodic boundary conditions. Chloride ions were added in order to compensate for the charges of the proteins. The rutile structure was kept frozen during the simulation, except the surface hydroxyl groups so that the Ti-O-H angle and the Ti-O and O-H bond lengths were constrained to their equilibrium values while the hydroxyl groups themselves were allowed rotate around the Ti-O bond. The rotational degrees of freedom can be seen dramatically influence on the binding modes and properties having a better possibility to direct interactions with the protein surface.[21, 22] Van der Waals interactions were handled by a twin-range cut-off method with the *rlist* and *rvdw* parameters set at 1.2 nm and 1.4 nm respectively. Long range electrostatic interactions were handled by particle mesh Ewald (PME) summation [23] with a cutoff of 1.2 nm for the separation of the direct and reciprocal space. Proteins were first equilibrated in aqueous solution without the rutile surface for an initial solution structure. Then the equilibrated protein – water boxes were placed on top of the rutile surface to form a rectangular box of  $116.94 \times 106.49 \times 99.000 \text{ \AA}^3$  for LF systems and  $103.95 \times 76.908 \times 99.000 \text{ \AA}^3$  for BMP-2 systems, respectively. Thereafter, the protein – Rutile systems did undergo a long equilibration. All the simulations were carried out in the NVT ensemble by using the Nosé-Hoover algorithm with a time constant of 0.1 ps and a reference temperature of 310 K.

The simulation systems consisted of one of the two proteins, the rutile surface, water and ions. For each combination of protein (LF, BMP2) and rutile atom charges (*low*, *original*, *high*) two simulations were performed: a reference simulation and a binding simulation. (both positions are shown in Figure S1 in Supporting Information) The proteins in the reference simulations were placed at a distance of 1.5 nm between the rutile surface and the most extended part of the protein surface. The start configurations of the binding simulations were created by moving the proteins closer to the rutile surface (see Figure 2 **Figure Captions**

**Figure 1.** Rutile (110) surface. See the text for details.

**Figure )**. The minimum distance between protein atoms and the rutile surface is initially set to about 0.4 nm, which is an effective range within the protein atoms and atoms in rutile have relatively large intermolecular interactions. [24-26] This is a compromise to obtain a binding state within a feasible computing time but still allows the protein relocate on the surface and freely undergo conformational changes. Table 2 shows a summary of all the MD simulations in this work.

After a proper equilibration of each system, the binding energies were calculated by subtracting the mean potential energy of the bound system from the mean potential energy of the reference system:

$$\Delta E_{\text{bind}} = \langle E_{\text{bound}} \rangle - \langle E_{\text{reference}} \rangle \quad (1)$$

The orientation of the protein with respect to the rutile surface was the same in all simulations. It was chosen visually based on the criteria that it would yield a large contact area between the protein and rutile. The sampling of the potential energy of the reference simulations was accelerated by placing positional restraints on the protein backbone atoms. The protein side chains were kept flexible in order for the protein to properly interact with water molecules. The protein movement was not restricted in any way in the binding simulations. A complete sampling of the binding of neither LF nor BMP2 to rutile by using atomistic MD simulations is currently not feasible due to the very slow protein dynamics and the long time scale of the binding processes. Coarse-graining or other types of simplifications would be necessary to follow the binding of a big protein to a surface. In this study, our primary aim is to estimate the relative binding energies depending on the surface character of the rutile (mimicked with changing the surface atom charges), rather than the absolute binding energies. From the binding energies we calculate the effect of the charges of the rutile atoms as the difference between the binding energies for different types of rutile surfaces:

$$\Delta \Delta E_{\text{bind},m-n} = \Delta E_{\text{bind},m} - \Delta E_{\text{bind},n} \quad (2)$$

where the indices  $m, n$  represent *low*, *original* or *high* rutile charges (See Table1).

## Results

### Structural Characterization

Visualizations of the simulations of the bound proteins show that both proteins interact favorably with the rutile surface. The proteins did not show any tendencies to depart from rutile, but rather moved even closer forming new contacts with the surface. These interactions between the proteins and rutile appeared to be stable throughout the simulations. Based upon this observation, we could assure both LF and



BMP2 as bound to rutile in all the binding simulations, *i.e.* both proteins bind to a rutile surface with *low*, *original* or *high* atomic charges. The variation in time of the distance between the center of mass of LF and BMP2 and the outermost atoms of the rutile surface are displayed in Figure 3

(A, B).

Figure 3A shows that LF stays close to the start distance in the simulation *LF<sub>high</sub>* but moves closer to rutile by  $\sim 0.1$  and  $\sim 0.2$  nm in the simulations *LF<sub>orig</sub>* and *LF<sub>low</sub>*, respectively. It seems that the type of the rutile surface affects the protein - rutile distance, with the shortest distance for the most hydrophobic surface and the longest distance for the most hydrophilic surface. BMP2 moves quickly closer to rutile in all simulations (see Figure 3B). However, the type of rutile surface seems to affect the protein - rutile distance for BMP2 as it did for LF. The distance is the longest in the simulation *BMP2<sub>high</sub>* and shortest in the simulation *BMP2<sub>low</sub>*.

The effect of the rutile hydrophobicity on the protein - rutile distance can also be seen in the number of water and protein atoms within a thin layer of 0.4 nm from the rutile surface. Closer analysis shows that the protein atoms replace water in the layer immediately above rutile in the simulations of the hydrophobic rutile surface (see Figure S2 in Supporting Information). The breakdown of water layer is similar to what has been observed in previous studies about the water molecules in protein-nonhydroxylated rutile interface.[22] On the other hand, when the rutile atomic charges are high, water can favorably compete with LF and BMP2 for the interaction with rutile. The rutile surface is then almost completely covered with water and the major part of the protein interacts with this hydration layer instead of interacting directly with rutile. The protein - rutile distance is therefore longer, as noted from Figure 3A and B. This effect can be seen in snapshots of the simulations, as in Figure 4.

The contacts between the proteins and rutile surface are described by the atom number fraction of total number contacted atoms as shown in Figure 5. The contacted atoms were divided into two groups: hydrophilic and hydrophobic by the residue properties they belong to. Gly, Ala, Val, Leu, Ile, Phe and Pro are defined as hydrophobic residues, while the others are hydrophilic. With the increasing of rutile hydrophilicity (rutile high charge amplitudes), the percentage of contacted

hydrophobic amino acids decreased. It can be seen that some of the peripheral hydrophobic amino acids interact with the hydrophobic surface rather than water, this way lowering the free energy. However, a number of hydrophilic amino acids, mainly arginine and glutamic acid for LF and BMP2 as well as lysine for BMP2, always have direct contact with rutile even at low rutile atomic charges.

We can observe from the graphs in Figure 4 that the distance between the center of mass of LF and rutile quickly settles to stable values while this process takes a longer time for BMP2 and does not seem to be quite finished at the end of the simulations. In the simulation *BMP2<sub>low</sub>* the distance between the protein center of mass and rutile is only ~1.4 nm after 50 ns, which corresponds to a decrease of 0.6 nm from the start distance of 2.0 nm. However, since the start distance between the protein surface and rutile was smaller than the decreasing center of mass distance, it is clear that the BMP2 have deformed, which is confirmed in backbone RMSD graphs. Figure 6 shows that LF maintains a structure close to its start structure in all simulations, giving RMSD values of 1.5 to 2.5 Å. BMP2 has low RMSD values in the simulations *BMP2<sub>orig</sub>* and *BMP2<sub>high</sub>* but deforms to a greater extent in the simulation *BMP2<sub>low</sub>*, where it reaches an RMSD value close to 5 Å, see Figure 6.

The sudden increase in the RMSD value of *BMP2<sub>low</sub>* after 25 ns can be traced to structural re-arrangements of residues 18 to 40 as well as 86 to 104 in the BMP2 monomer that was positioned closer to the rutile surface. Figure 7 displays the structure of BMP2 before and after the deformation. The deformation of the protein can be clearly seen when comparing these figures with the structure of the BMP2 monomer colored white. The crystal structure of the BMP2 monomer has a slight curvature that inhibits full contact with the flat rutile surface. The deformation of the monomer resulted in a more flat protein structure and the protein - rutile contact area was thereby increased.

Due to the long time scale required to follow the complete binding process, it is not possible to say if LF would go through a similar deformation in the simulation *LF<sub>low</sub>* and if BMP2 would lose more of its native structure in the simulation *BMP2<sub>low</sub>*. However, such deformations seemed to be more likely when the rutile surface was hydrophobic rather than hydrophilic based upon the greater number of protein – rutile contacts in *LF<sub>low</sub>* and *BMP2<sub>low</sub>*.

### Protein Binding Energies

The internal energy of binding was calculated for both LF and BMP2 in combination with all three types of rutile surfaces. The potential energies were sampled every ps in all simulations. Based on visual observations of the simulations and the initial trends found in the data, the first 9 ns were taken as equilibration for both the reference simulations and the binding simulations and the data therefore represents times  $t > 9$  ns. Distribution functions of the system potentials of the LF simulations are displayed in Figure 8.

The system potential energy is shifted towards lower values when LF binds to the rutile surface, indicating that the protein binding is energetically favored for all three types of rutile surface. The binding energies for the three LF systems are displayed in Table 3. It should be remembered that the absolute values of the binding energies are not necessarily correct due to the use of positional restraints on the proteins in the reference simulations and only corresponds to binding of one side of the protein. Still, a clear and consistent trend can be seen in the all three systems. The absolute value of the binding energy decreases with higher atomic charge amplitudes of rutile, *i.e.* the binding is stronger to a more hydrophobic surface. However, note that the standard deviations of the binding energies are relatively large. In the third column of Table 3, the *LF<sub>low</sub>* system has been used as a reference to which the other two systems are compared. It can be seen that the binding of LF to rutile is less exothermic by 70 and 240 kJ/mol in *LF<sub>orig</sub>* and *LF<sub>high</sub>*, respectively, than in the *LF<sub>low</sub>* system.

The corresponding distribution functions of the system potential energies for the BMP2 systems are displayed in Figure 9. The smaller size of the BMP2 protein gave the possibility for longer simulations and better sampling compared to that for lactoferrin. This resulted in smoother distribution functions for BMP2 but the trend in the binding energies, as shown in Table 4, is the same as for LF. The trend is consistent between the simulations with the *low original* and *high* rutile surfaces as BMP2. The relative binding energies,  $\Delta\Delta E_{\text{bind,m-n}}$ , in Table 3 and Table 4 were compared among the BMP2 and LF systems. We can see that both proteins exhibit the most exothermic binding to the hydrophobic rutile surface “*low*”. The relative binding energies are also similar in amplitude – roughly +100 -150 kJ/mol when changing the rutile surface from *low*  $\rightarrow$  *orig.*  $\rightarrow$  *high*.

## Discussion

Binding of human LactoFerrin and human Bone Morphogenetic Protein-2 to hydroxylated TiO<sub>2</sub> rutile surfaces has been studied using MD simulations. The main purpose was to observe if the hydrophobicity of the rutile surface affects the protein binding process. The hydrophobicity of rutile was changed simply by down-scaling or up-scaling the charges of the rutile atoms, while making sure to keep the charge neutrality of the surface as a whole. Both the hydrophobic and hydrophilic amino acids interact with the rutile surface. Some hydrophilic charged residues including arginine, glutamic acid and lysine, were found to have strong interactions in all of the studied surfaces. It proves that strong electrostatic interactions with titanium dioxide surface are responsible for the binding, which has also been reported in literature.[14, 27, 28] Moreover, clear protein deformation was observed when proteins bind to the most hydrophobic surface, which is in agreement with both computational and experimental studies.[3, 13] BMP-2 has a higher degree of deformation and stronger binding compared with LF when it is bound to the more hydrophobic rutile surface. For BMP-2, one of its monomers underwent large structural rearrangements in order to increase its contact area with rutile, which has also been found when its monomer was bound to graphite.[29] In contrast, LF shows a less deformed structure when bonded, which may be attributed to its inherent less flexibility due to its large molecular weight and more compact structure compared with the BMP-2 dimer. Protein binding to the more hydrophilic surfaces was markedly different. Water competes with the proteins for the interaction with the hydrophilic rutile surface, which results in rutile being almost completely covered with water molecules. The proteins are pushed further away from rutile and most contacts with rutile must occur indirectly via interactions with the water layer on top of rutile surface. However, some direct contacts also occur but these are dominated by charged amino acids.

The longer protein – rutile distance and the fewer contacts between the protein and the rutile surface for a hydrophilic rutile surface affected the binding energies. Binding to the hydrophobic “*low*” rutile surface resulted in the largest decrease in the system potential, while binding to the more hydrophilic “*original*” and “*high*” surfaces resulted in successively smaller decreases in the system potential energy. This trend was the same between both proteins. We therefore conclude that, from a purely

energetic perspective, both LF and BMP2 have a stronger binding to a more hydrophobic rutile surface. However the Gibbs free energy of binding should have been calculated rather than binding energies but such an analysis was simply not possible for these large systems, containing on the order of 100 000 atoms. Obviously it is difficult to conclude if the entropic effect to the binding is favorable or unfavorable.[30-32] The entropy gain caused by water mobility and displacement will become compensated by a considerable loss of entropy due to reduced protein mobility when it is restricted on a two-dimensional surface.[33] However, we can argue that the entropic term would in fact “favor” the protein binding to hydrophobic rutile surfaces rather than to hydrophilic involving a larger entropy gain. Both LF and BMP2 replace water molecules at the rutile surface to a much higher degree for the hydrophobic surface. These water molecules, first removed from the relatively immobile hydration layer on the rutile surface, will successively regain the mobility of bulk water and to a smaller extent even while hydrating the protein. This gives a net entropic gain to the hydrophobic surface over hydrophilic surface. At the same time, the hydrophobic amino acids can also more freely move towards the hydrophobic interface. This overall entropy increase for both water and protein with a simultaneous minor change in enthalpy should in turn lower the free energy. Although we cannot at the moment prove this with calculations, we hope when the free energy calculations for protein adsorbed on metal surface becomes reality they would give us right.

## Conclusions

Interactions of two proteins; human lactoferrin (LF) with antibacterial activity and a part of the immune system of our body and human Bone Morphogenetic Protein-2 (BMP2) which is important in development of bones and cartilage to hydroxylated TiO<sub>2</sub> rutile (110) surface have been studied using MD simulations to find out the effect of the hydrophobicity of the rutile surface on the protein binding process. The hydrophobic and hydrophilic characters, respectively, were created by adjusting the rutile atomic charges. For the both proteins the binding to the hydrophobic rutile surface was through a direct contact between the protein and rutile via both hydrophobic and hydrophilic amino acids. While binding this way the both proteins

underwent structural rearrangements, observed more strongly in BMP2. In binding to the hydrophilic rutile surface there was a hydration layer of water molecules between the rutile surface and the proteins. Both LF and BMP2 exhibited a higher binding strength to the hydrophobic rutile surfaces than to the hydrophilic surfaces.

### **Acknowledgements**

This work has been supported work by the Swedish Science Council. Computations were performed on resources provided by the Swedish National Infrastructure for Computing (SNIC) at PDC, HPC2N, and NSC.

## References

- [1] Costa D, Garrain PA, Baaden M. Understanding small biomolecule-biomaterial interactions: A review of fundamental theoretical and experimental approaches for biomolecule interactions with inorganic surfaces. *J Biomed Mater Res A*. 2013;101A:1210-22.
- [2] Skelton AA, Liang TN, Walsh TR. Interplay of sequence, conformation, and binding at the peptide-titania interface as mediated by water. *ACS Appl Mater Inter*. 2009;1:1482-91.
- [3] Utesch T, Daminelli G, Mroginski MA. Molecular dynamics simulations of the adsorption of bone morphogenetic protein-2 on surfaces with medical relevance. *Langmuir*. 2011;27:13144-53.
- [4] Wu CY, Chen MJ, Xing C. Molecular understanding of conformational dynamics of a fibronectin module on rutile (110) surface. *Langmuir*. 2010;26:15972-81.
- [5] Jose JC, Sengupta N. Molecular dynamics simulation studies of the structural response of an isolated  $\alpha$ 1(I)-collagen monomer localized in the vicinity of the hydrophilic  $\text{TiO}_2$  surface. *Eur Biophys J Biophys*. 2013;42:487-94.
- [6] Zhang HP, Lu X, Leng Y, Watari F, Weng J, Feng B, et al. Effects of aqueous environment and surface defects on arg-gly-asp peptide adsorption on titanium oxide surfaces investigated by molecular dynamics simulation. *J Biomed Mater Res A*. 2011;96A:466-76.
- [7] Roach P, Eglin D, Rohde K, Perry CC. Modern biomaterials: A review-bulk properties and implications of surface modifications. *J Mater Sci-mater M*. 2007;18:1263-77.
- [8] Teughels W, Van Assche N, Sliepen I, Quirynen M. Effect of material characteristics and/or surface topography on biofilm development. *COIR*. 2006;17 Suppl 2:68-81.
- [9] Dettin M, Bagno A, Gambaretto R, Iucci G, Conconi MT, Tuccitto N, et al. Covalent surface modification of titanium oxide with different adhesive peptides: Surface characterization and osteoblast-like cell adhesion. *J Biomed Mater Res A*. 2009;90:35-45.
- [10] Chen X, Mao SS. Titanium dioxide nanomaterials: Synthesis, properties, modifications, and applications. *Chem Rev*. 2007;107:2891-959.
- [11] Arima Y, Iwata H. Effects of surface functional groups on protein adsorption and subsequent cell adhesion using self-assembled monolayers. *J Mater Chem*. 2007;17:4079-87.
- [12] MacDonald DE, Deo N, Markovic B, Stranick M, Somasundaran P. Adsorption and dissolution behavior of human plasma fibronectin on thermally and chemically modified titanium dioxide particles. *Biomaterials*. 2002;23:1269-79.
- [13] Roach P, Farrar D, Perry CC. Interpretation of protein adsorption: Surface-induced conformational changes. *J Am Chem Soc*. 2005;127:8168-73.
- [14] Kang Y, Li X, Tu YQ, Wang Q, Agren H. On the mechanism of protein adsorption onto hydroxylated and nonhydroxylated  $\text{TiO}_2$  surfaces. *J Phys Chem C*. 2010;114:14496-502.

- [15] Wu CY, Chen MJ, Skelton AA, Cummings PT, Zheng T. Adsorption of arginine-glycine-aspartate tripeptide onto negatively charged rutile (110) mediated by cations: The effect of surface hydroxylation. *Acs Appl Mater Inter*. 2013;5:2567-79.
- [16] Tomita M, Wakabayashi H, Shin K, Yamauchi K, Yaeshima T, Iwatsuki K. Twenty-five years of research on bovine lactoferrin applications. *Biochimie*. 2009;91:52-7.
- [17] Bandura AV, Kubicki JD. Derivation of force field parameters for tio<sub>2</sub>-h<sub>2</sub>o systems from a initio calculations. *J Phys Chem B*. 2003;107:11072-81.
- [18] Predota M, Bandura AV, Cummings PT, Kubicki JD, Wesolowski DJ, Chialvo AA, et al. Electric double layer at the rutile (110) surface. 1. Structure of surfaces and interfacial water from molecular dynamics by use of ab initio potentials. *J Phys Chem B*. 2004;108:12049-60.
- [19] Hess B, Kutzner C, van der Spoel D, Lindahl E. Gromacs 4: Algorithms for highly efficient, load-balanced, and scalable molecular simulation. *J Chem Theory Comput*. 2008;4:435-47.
- [20] Jorgensen WL, Chandrasekhar J, Madura JD, Impey RW, Klein ML. Comparison of simple potential functions for simulating liquid water. *J Chem Phys*. 1983;79:926-35.
- [21] Qiao BF, Sega M, Holm C. Properties of water in the interfacial region of a polyelectrolyte bilayer adsorbed onto a substrate studied by computer simulations. *Phys Chem Chem Phys*. 2012;14:11425-32.
- [22] Yang C, Peng CW, Zhao DH, Liao CY, Zhou J, Lu XH. Molecular simulations of myoglobin adsorbed on rutile (110) and (001) surfaces. *Fluid Phase Equilib*. 2014;362:349-54.
- [23] Essmann U, Perera L, Berkowitz ML, Darden T, Lee H, Pedersen LG. A smooth particle mesh ewald method. *J Chem Phys*. 1995;103:8577-93.
- [24] Panos M, Sen TZ, Ahunbay MG. Molecular simulation of fibronectin adsorption onto polyurethane surfaces. *Langmuir*. 2012;28:12619-28.
- [25] Zhang JQ, Sun TY, Liang LJ, Wu T, Wang Q. Drug promiscuity of p-glycoprotein and its mechanism of interaction with paclitaxel and doxorubicin. *Soft Matter*. 2014;10:438-45.
- [26] Qiao BF, Cerda JJ, Holm C. Atomistic study of surface effects on polyelectrolyte adsorption: Case study of a poly(styrenesulfonate) monolayer. *Macromolecules*. 2011;44:1707-18.
- [27] Monti S, Carravetta V, Zhang WH, Yang JL. Effects due to interadsorbate interactions on the dipeptide/tio<sub>2</sub> surface binding mechanism investigated by molecular dynamics simulations. *J Phys Chem C*. 2007;111:7765-71.
- [28] Xu Z, Liu XW, Ma YS, Gao HW. Interaction of nano-tio<sub>2</sub> with lysozyme: Insights into the enzyme toxicity of nanosized particles. *Environ Sci Pollut R*. 2010;17:798-806.
- [29] Mucksch C, Urbassek HM. Adsorption of bmp-2 on a hydrophobic graphite surface: A molecular dynamics study. *Chem Phys Lett*. 2011;510:252-6.



- [30] Friedman R, Nachliel E, Gutman M. Fatty acid binding proteins: Same structure but different binding mechanisms? Molecular dynamics simulations of intestinal fatty acid binding protein. *Biophys J.* 2006;90:1535-45.
- [31] Mijajlovic M, Penna MJ, Biggs MJ. Free energy of adsorption for a peptide at a liquid/solid interface via nonequilibrium molecular dynamics. *Langmuir.* 2013;29:2919-26.
- [32] Lin FY, Chen WY, Hearn MTW. Microcalorimetric studies on the interaction mechanism between proteins and hydrophobic solid surfaces in hydrophobic interaction chromatography: Effects of salts, hydrophobicity of the sorbent, and structure of the protein. *Anal Chem.* 2001;73:3875-83.
- [33] Ben-Tal N, Honig B, Bagdassarian CK, Ben-Shaul A. Association entropy in adsorption processes. *Biophys J.* 2000;79:1180-7.

**Figure Captions**

**Figure 1.** Rutile (110) surface. See the text for details.

**Figure 2.** Start configurations of the LF (upper) and BMP2 (lower) binding simulations.

**Figure 3.** The distance between the centre of mass of protein and the rutile surface. (A) LF (B) BMP2.

**Figure 4.** Snapshot from the simulation *LF<sub>low</sub>* (upper) and *LF<sub>high</sub>* (lower).

**Figure 5.** The fraction of LF (left) and BMP2 (right) atoms within 0.4 nm of rutile that can be classified as belonging to hydrophobic vs. hydrophilic amino acids.

**Figure 6.** Backbone RMSD for LF (left) and BMP2 (right) in the binding simulations.

**Figure 7.** BMP2<sub>low</sub> in simulation before (upper) and after (lower) adsorption.

**Figure 8.** System potential distribution functions for the LF system.

**Figure 9.** System potential energy distribution functions for the BMP2 system.

**Table 1.** Atomic charges of the three types of rutile surfaces.

<b>Atom</b>	<b><i>low</i></b>	<b><i>original</i></b>	<b><i>high</i></b>
Ti	1.098	2.196	3.0744
O	-0.549	-1.098	-1.5372
Obp	-0.518	-1.035	-1.4495
Hbp	0.243	0.486	0.6804
Oth	-0.504	-1.008	-1.4112
Hth	0.230	0.459	0.6431

**Table 2.** Descriptions of the simulations.

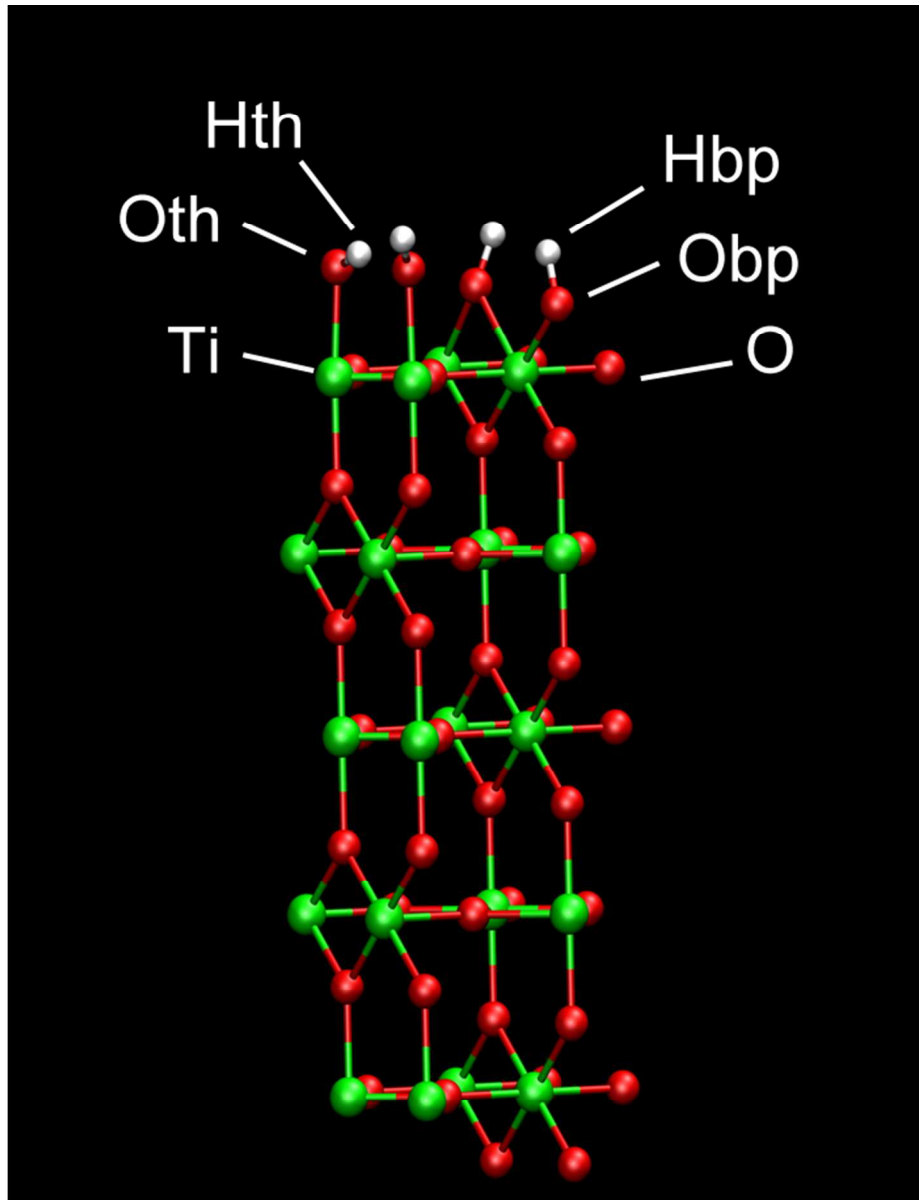
Simulation Name	Protein	Simulation Type	Charge of the rutile atoms	Simulation length
<b>LF low ref</b>	Lactoferrin	Reference simulation	$0.5 \times \textit{Original}$	18 ns
<b>LF low</b>	Lactoferrin	Binding simulation	$0.5 \times \textit{Original}$	27 ns
<b>LF orig ref</b>	Lactoferrin	Reference simulation	<i>Original</i>	18 ns
<b>LF orig</b>	Lactoferrin	Binding simulation	<i>Original</i>	27 ns
<b>LF high ref</b>	Lactoferrin	Reference simulation	$1.4 \times \textit{Original}$	18 ns
<b>LF high</b>	Lactoferrin	Binding simulation	$1.4 \times \textit{Original}$	27 ns
<b>BMP2 low ref</b>	BMP-2	Reference simulation	$0.5 \times \textit{Original}$	40 ns
<b>BMP2 low</b>	BMP-2	Binding simulation	$0.5 \times \textit{Original}$	50 ns
<b>BMP2 orig ref</b>	BMP-2	Reference simulation	<i>Original</i>	40 ns
<b>BMP2 orig</b>	BMP-2	Binding simulation	<i>Original</i>	56 ns
<b>BMP2 high ref</b>	BMP-2	Reference simulation	$1.4 \times \textit{Original}$	40 ns
<b>BMP2 high</b>	BMP-2	Binding simulation	$1.4 \times \textit{Original}$	50 ns

**Table 3.** The protein binding energies of the LF systems.

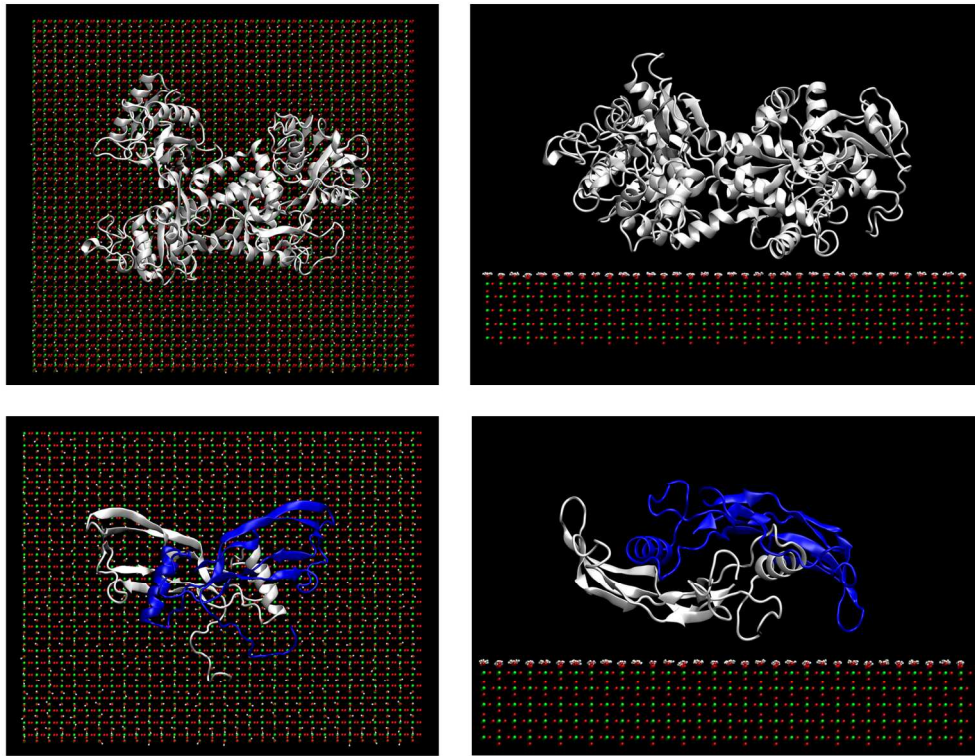
<b>System</b>	$\Delta E_{\text{bind}}$ [kJ/mol]	$\Delta\Delta E_{\text{bind,m-low}}$ [kJ/mol]
<b>LFlow</b>	$-360 \pm 60$	0
<b>LForig</b>	$-290 \pm 40$	+70
<b>LFhigh</b>	$-120 \pm 70$	+240

**Table 4.** The protein binding energies of the BMP2 systems.

<b>System</b>	$\Delta E_{\text{bind}}$ <b>[kJ/mol]</b>	$\Delta\Delta E_{\text{bind,m-low}}$ <b>[kJ/mol]</b>
<b>BMP2<sub>low</sub></b>	-2760 ± 40	0
<b>BMP2<sub>orig</sub></b>	-2650 ± 25	+110
<b>BMP2<sub>high</sub></b>	-2430 ± 100	+330

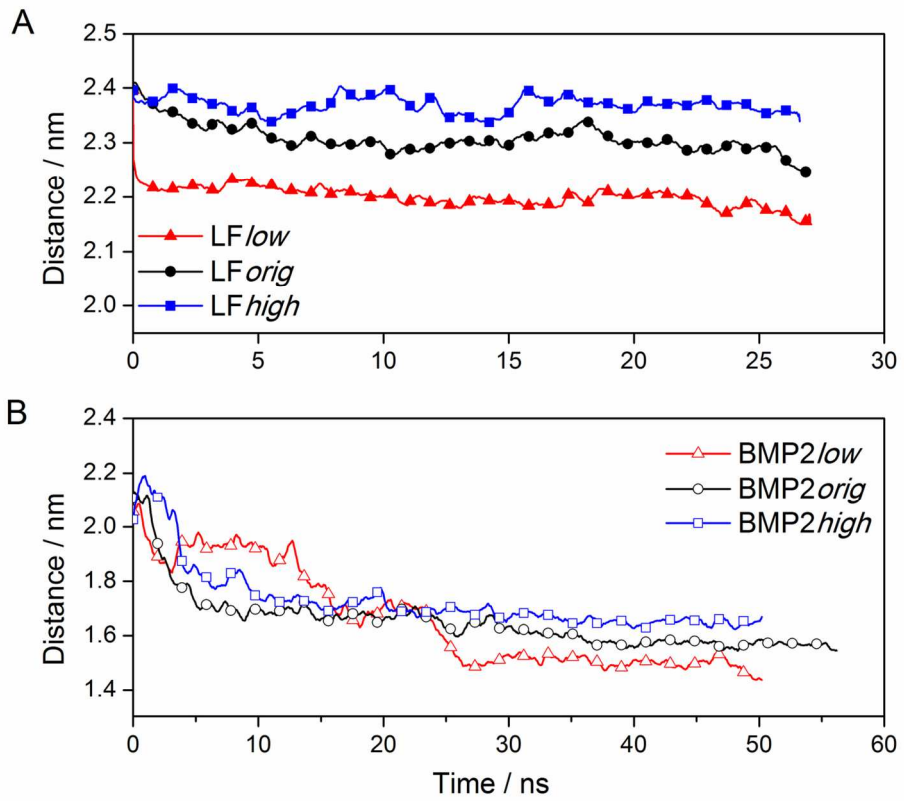


Rutile (110) surface  
59x77mm (300 x 300 DPI)

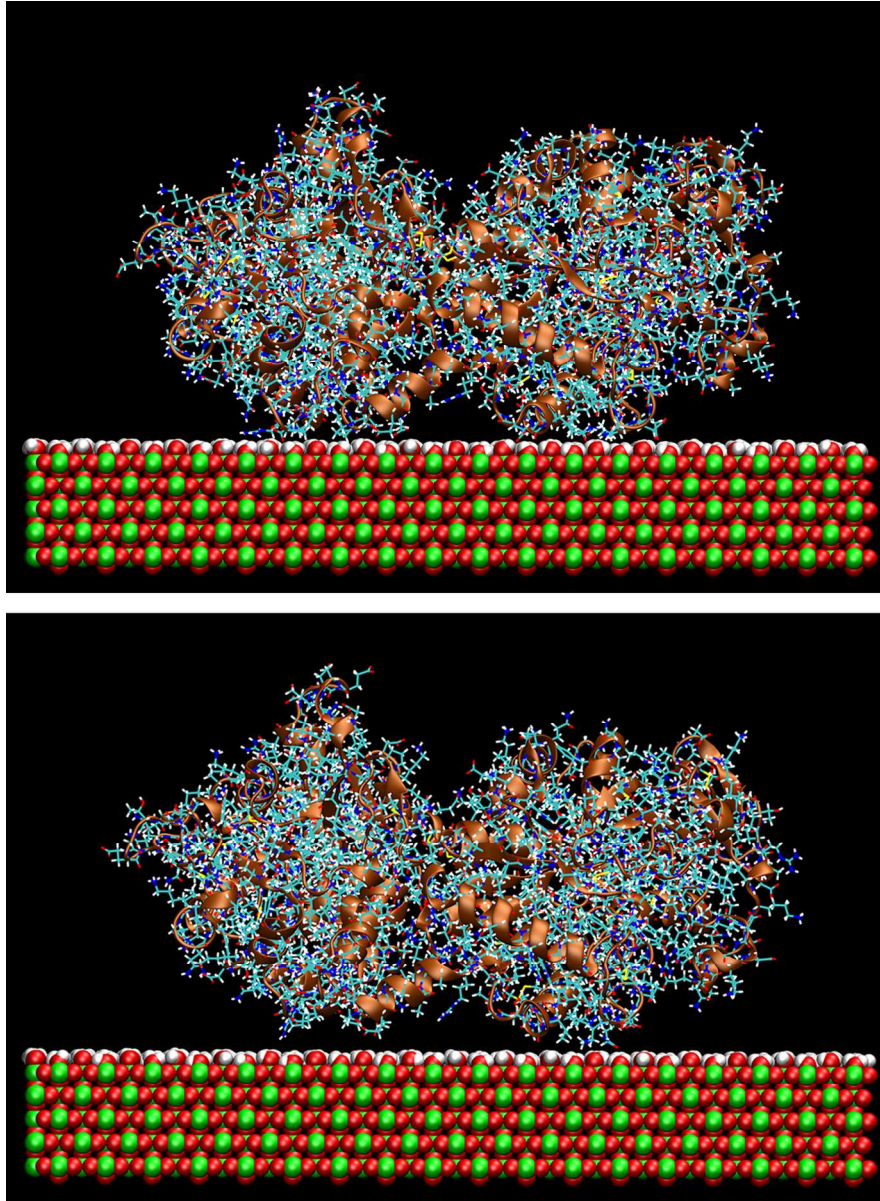


157x123mm (300 x 300 DPI)

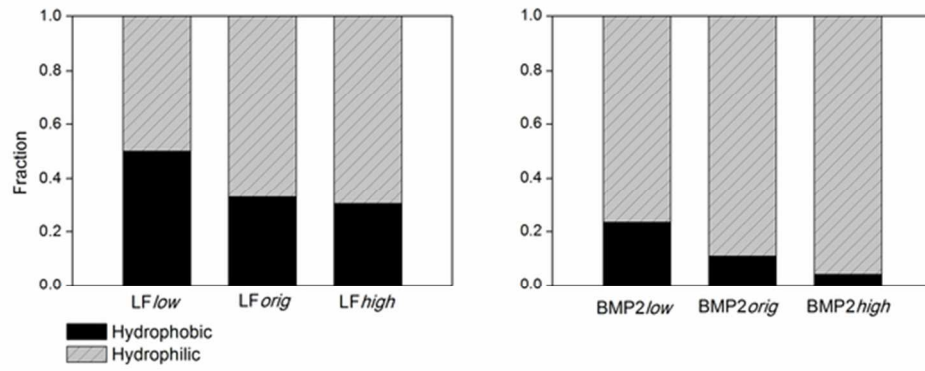




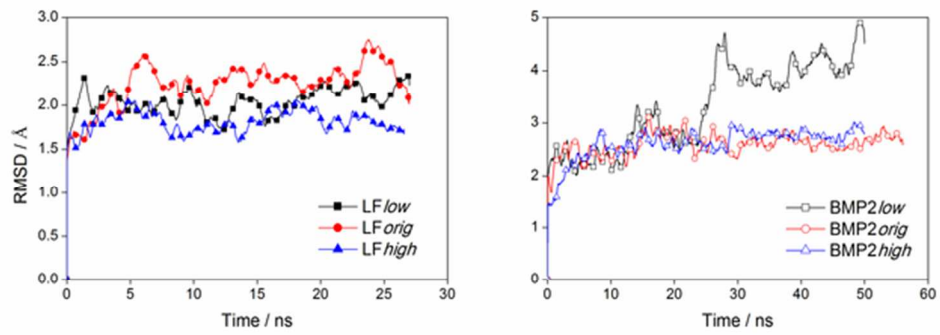
128x109mm (300 x 300 DPI)



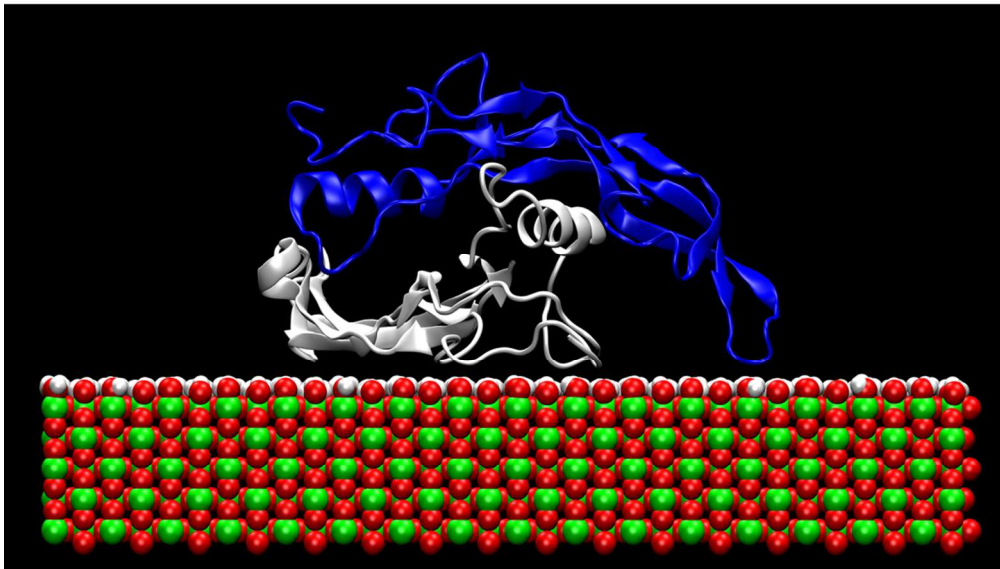
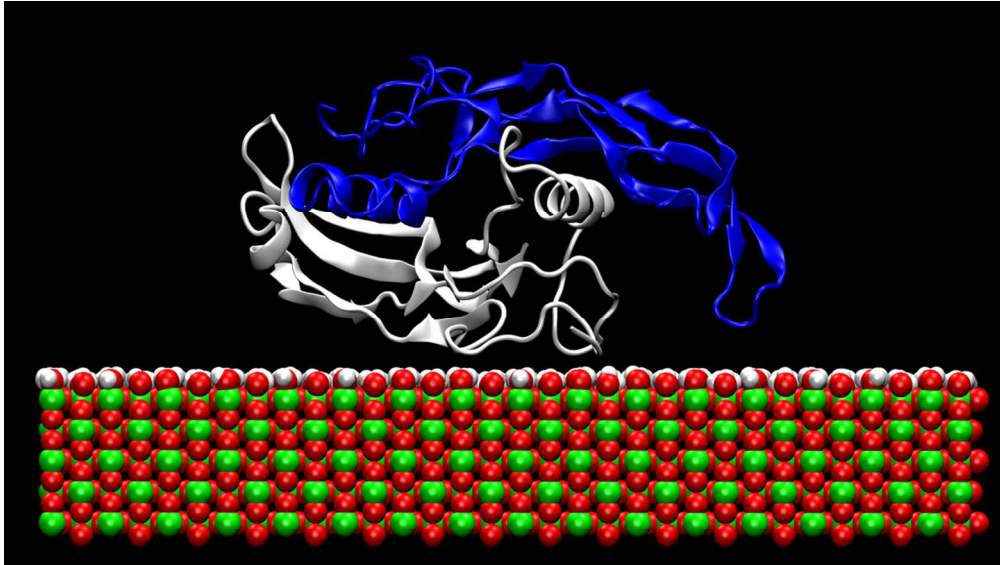
121x166mm (300 x 300 DPI)



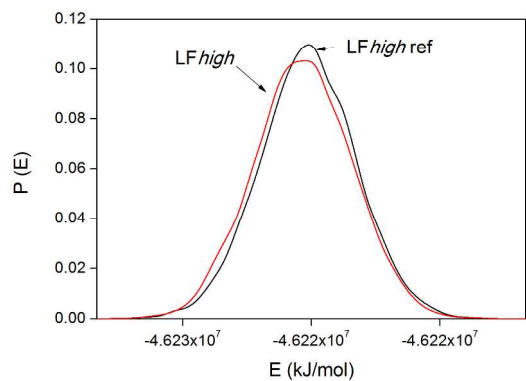
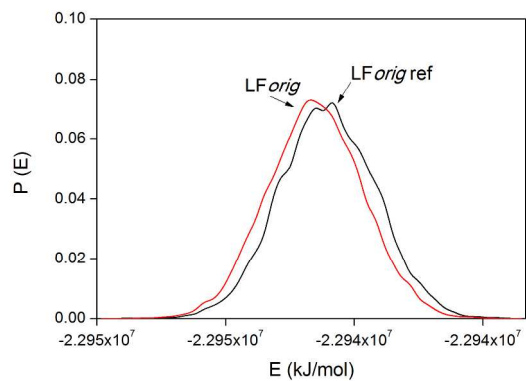
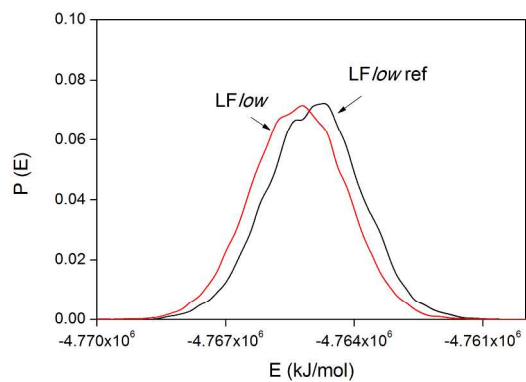
57x22mm (300 x 300 DPI)



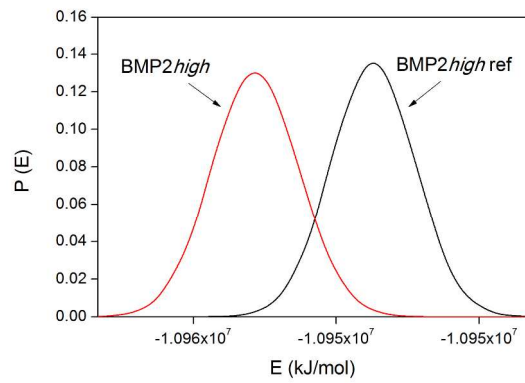
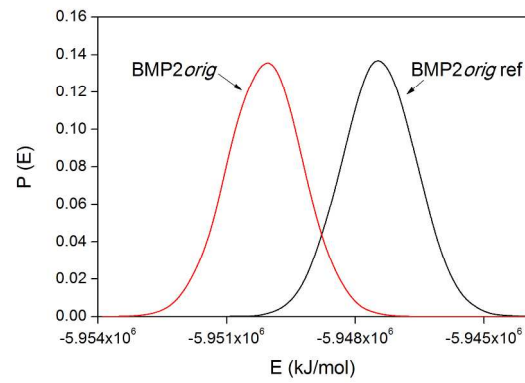
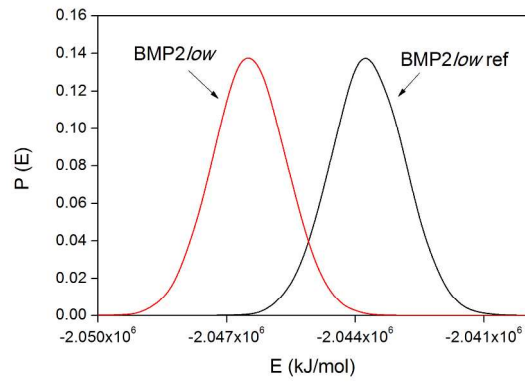
56x21mm (300 x 300 DPI)



99x115mm (300 x 300 DPI)

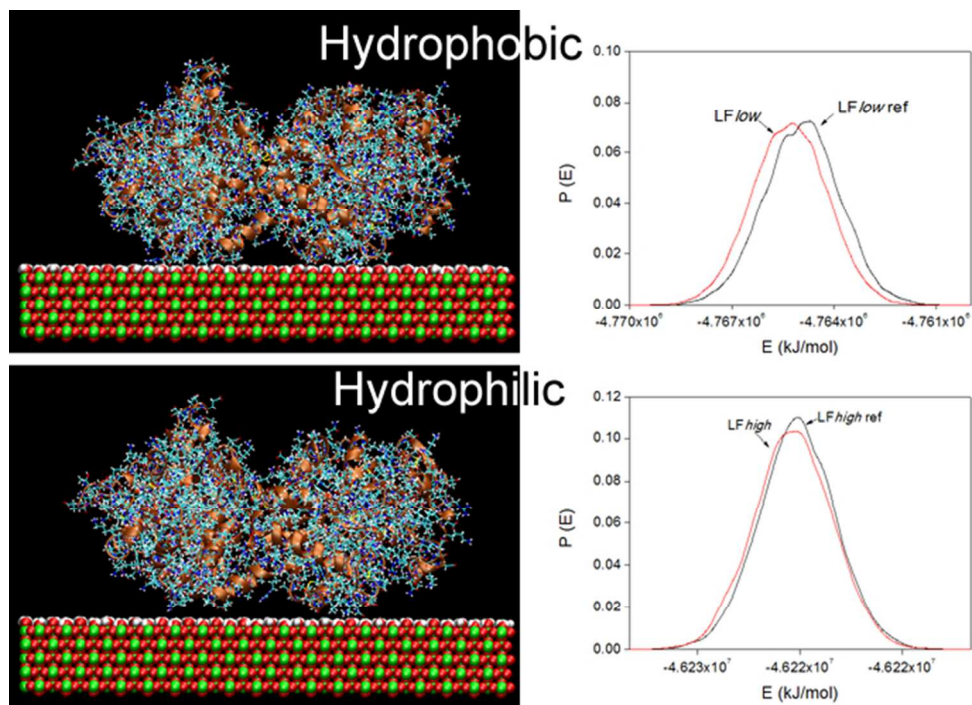


178x374mm (300 x 300 DPI)



178x374mm (300 x 300 DPI)





Adhesion of Lactoferrin and Bone Morphogenetic Protein-2 to a Rutile Surface: Dependence on the Surface Hydrophobicity.

60x41mm (300 x 300 DPI)